ISSN : 0974 - 7486 Volume 10 Issue 12

Materials Science

An Indian Journal

Full Paper

MSAIJ, 10(12), 2014 [515-521]

Pressure induced structural phase transition and elastic properties of barium and cerium selenide

Kuldeep Kholiya[1]*, Jeewan Chandra[2], Monika Goyal[3], B.R.K.Gupta[3]

[1]Department of Applied Science, B.T. Kumaon Institute of Technology, Dwarahat, 263653, Uttarakhand, (INDIA)

[2]Department of Applied Science, G.B.P. Engineering College, Ghurdauri, Pauri, Garhwal, 246194, Uttarakhand, (INDIA)

[3]Department of Physics, GLA University, Mathura, (INDIA)

E-mail : kuldeep_phy1@rediffmail.com

PACS : 61.50.Ks; 61.50.Lt

ABSTRACT

In the present investigation the B1-B2 structural phase transition and elastic properties of BaSe and CeSe has been predicted using the simple potential model considered third nearest neighbor interaction. The calculated values of B1-B2 phase transition pressure, equation of state (Compression curve), bulk modulus, its first order pressure derivative and second order elastic constants are given along with the available experimental and other theoretical values. The results achieved in the present study are found in good agreement with the available experimental data.

KEYWORDS

B1 – B2 phase transition;
High pressure;
Cohesive energy;
Potential model.

INTRODUCTION

At ambient pressure and temperature, BaSe and CeSe exhibit NaCl-type structure, however with the application of pressure they undergo first order phase transition from the sixfold-coordinated NaCl-type (B1 structure) to the eightfold-coordinated CsCl-type (B2 structure). The high pressure X-ray diffraction studies suggest the B1-B2 phase transition pressure of 6.0 and 20.0 GPa for BaSe and CeSe, respectively[1,2].

In the past years, many efforts were made to interpret the experimental results[1-4] regarding phase transition, elastic and cohesive properties in the BaSe and CeSe using a variety of theoretical models[5-15]. Most of these approaches used different methods of band structure calculations, such as scalar relativistic full potential-linearized augmented plane wave (FP-LAPW) approach within the framework of density functional theory[5], self- consistent linearized augmented plane wave (LAPW)[6], tight-binding linear muffin-tin orbitals (TB-LMTO)[7], linear muffin-tin orbitals (LMTO)[8], augmented-spherical wave method within the local-density approximation (LDA-ASW)[9], full-potential augmented plane wave plus local orbital (FP-APW + lo) method[10,11], self-interaction corrected local spin-density (SIC-LSD) approximation[12], as well as the potential model[13-15]. However, some of these theories predict the transition pressure, compression curve and cohesive properties, close to the experimental findings. But these calculations require rigorous computational work.

In view of above facts, the aim of the present study

Full Paper

is to formulate the simple and straightforward potential model to determine the B1-B2 phase transition pressure, the equation of state (compression curve), the elastic and cohesive properties of BaSe and CeSe.

METHOD OF ANALYSIS

The Gibbs free energy is defined as:

$$G = U + PV - TS \quad (1)$$

Here U is the lattice energy and V and S are respectively, the volume and vibrational entropy at pressure P, and temperature T. Considering that the entropy (S) has a constant value at room temperature (T), for both the phases, the Gibbs free energy for B1 and B2 phases may be given as follows[16,17]:

$$G_{B1}(r) = U_{B1}(r) + 2(r)^3 P - TS \quad (2)$$

and

$$G_{B2}(r^1) = U_{B2}(r^1) + \frac{8(r^1)^3 P}{3\sqrt{3}} - TS \quad (3)$$

Here, $2(r)^3 = V_{B1}$ and $\frac{8(r^1)^3}{3\sqrt{3}} = V_{B2}$.

Lattice energy, which includes long range Coulomb interaction and short range repulsive energy up to third nearest neighbor makes the cohesive energies, for B1 and B2 phases as follows[16,17]:

$$U_{B1}(r) = -\left(\frac{\alpha_M Z^2 e^2}{4\pi\varepsilon_0 r}\right) + 6b_{B1}\exp\left(\frac{-r}{\rho_{B1}}\right) + 12b_{B1}\exp\left(\frac{-\sqrt{2}r}{\rho_{B1}}\right) + 8b_{B1}\exp\left(\frac{-\sqrt{3}r}{\rho_{B1}}\right) \quad (4)$$

$$U_{B2}(r^1) = -\left(\frac{\alpha_M^1 Z^2 e^2}{4\pi\varepsilon_0 r^1}\right) + 8b_{B2}\exp\left(\frac{-r^1}{\rho_{B2}}\right) + 6b_{B2}\exp\left(\frac{-2r^1}{\sqrt{3}\rho_{B2}}\right) + 12b_{B2}\exp\left(\frac{-2\sqrt{2}r^1}{\sqrt{3}\rho_{B2}}\right) \quad (5)$$

Here, r and r^1, are the nearest-neighbor separations; α_M and α_M^1 are the Modelung constants; ρ_{B1} and ρ_{B2} are the range parameters; b_{B1} and b_{B2} are the strength parameters in B1 and B2 phases, respectively. At different pressure, to determine the value of Gibbs free energy for B1 and B2 phases, $r(r^1)$ is calculated by minimizing the Gibbs free energy at that pressure and the phase transition pressure is the pressure at which the difference of Gibbs free energy for two phases i.e. dG ($= G_{B2}$-G_{B1}) becomes zero. This requires the determination of range and strength parameter in B1 and B2 phases. For B1 phase, the range and the strength parameter may be determined from the thermodynamic condition of bulk modulus i.e. $B_{01} = V_{01}\left(d^2U_{B1}(r)/dV_1^2\right)_{r=r_0}$, and the equilibrium condition i.e. $\left[dU_{B1}(r)/dr\right]_{r=r_0} = 0$ which gives

$$B_{01} = \frac{\alpha_M Z^2 e^2}{4\pi\varepsilon_0 \times 9r_0^4}\left[\frac{r_0}{2\rho_{B1}}\left\{\frac{\exp\left(\frac{-r_0}{\rho_{B1}}\right) + 4\exp\left(\frac{-\sqrt{2}r_0}{\rho_{B1}}\right)}{\exp\left(\frac{-r_0}{\rho_{B1}}\right) + 2\sqrt{2}\exp\left(\frac{-\sqrt{2}r_0}{\rho_{B1}}\right)} + 4\exp\left(\frac{-\sqrt{3}r_0}{\rho_{B1}}\right)\right\} + \frac{4}{\sqrt{3}}\exp\left(\frac{-\sqrt{3}r_0}{\rho_{B1}}\right)\right\} - 1\Bigg] \quad (6)$$

and

$$b_{B1} = \frac{\alpha_M Z^2 e^2 \rho_{B1}}{4\pi\varepsilon_0 \times 6r_0^2\left[\exp\left(\frac{-r_0}{\rho_{B1}}\right) + 2\sqrt{2}\exp\left(\frac{-\sqrt{2}r_0}{\rho_{B1}}\right) + \frac{4}{\sqrt{3}}\exp\left(\frac{-\sqrt{3}r_0}{\rho_{B1}}\right)\right]} \quad (7)$$

As the strength parameter determines the strength of the potential and at the phase transition the coordination number (number of the nearest neighbors) increases from 6 to 8 so it is obvious that the value of strength parameter will also increase for B2 phase. For B2 phase the strength parameter may be given as[18,19]

$$b_{B2} = \frac{8}{6} \times b_{B1} \quad (8)$$

While the range parameter is a measure of the range of the potential so its value for B2 phase decreases as at the B1-B2 phase transition the nearest neighbor distance increases. The value of range parameter for B2

phase (ρ_{B2}) may be calculated from the minima of the Gibbs free energy whereas the interionic separation (r^1) can be calculated with the help of volume collapse at the phase transition pressure[19].

The bulk modulus and the pressure derivative of the bulk modulus for B1 and B2 phases are calculated by fitting *P-V* data to the Vinet equation of state[20], given as:

$$P = 3\left[1-\left(\frac{V}{V_0}\right)^{1/3}\right]\times\exp\left[\frac{3\left(B_0^1-1\right)}{2}\times\left\{1-\left(\frac{V}{V_0}\right)^{1/3}\right\}\right]\times B_0\times\left(\frac{V_0}{V}\right)^{2/3} \quad (9)$$

and then applying the method of least square fit.

Further to calculate the elastic constants (C_{11}, C_{12}, C_{44}) for B1 phase, we have partition them into the contributions from Coulombic and short range forces i.e.

$$C_{ij} = C_{ij}^{Coul} + C_{ij}^{SR} \quad (10)$$

The Coulombic contribution in the elastic constants may be given as[19,21]

$$C_{11}^{Coul} = -\frac{2.55604e^2Z^2}{4\pi\varepsilon_0\times 2r^4} \quad (11)$$

$$C_{12}^{Coul} = \frac{0.11298e^2Z^2}{4\pi\varepsilon_0\times 2r^4} \quad (12)$$

$$C_{44}^{Coul} = \frac{1.27802e^2Z^2}{4\pi\varepsilon_0\times 2r^4} \quad (13)$$

The short-range (SR) contributions considered up to third nearest neighbor interactions are:

$$C_{11}^{SR} = \frac{1}{r}\left(\frac{d^2U_{FNN}}{dR^2}\right)_{R=r} + \frac{2}{r}\left(\frac{d^2U_{SNN}}{dR^2}\right)_{R=\sqrt{2}r} + \frac{\sqrt{2}}{r^2}\left(\frac{dU_{SNN}}{dR}\right)_{R=\sqrt{2}r} + \frac{4}{3r}\left(\frac{d^2U_{TNN}}{dR^2}\right)_{R=\sqrt{3}r} + \frac{8}{3\sqrt{3}r^2}\left(\frac{dU_{TNN}}{dR}\right)_{R=\sqrt{3}r} \quad (14)$$

$$C_{12}^{SR} = -\frac{1}{r^2}\left(\frac{dU_{FNN}}{dR}\right)_{R=r} + \frac{1}{r}\left(\frac{d^2U_{SNN}}{dR^2}\right)_{R=\sqrt{2}r} - \frac{5}{\sqrt{2}r^2}\left(\frac{dU_{SNN}}{dR}\right)_{R=\sqrt{2}r} + \frac{4}{3r}\left(\frac{d^2U_{TNN}}{dR^2}\right)_{R=\sqrt{3}r} - \frac{16}{3\sqrt{3}r^2}\left(\frac{dU_{TNN}}{dR}\right)_{R=\sqrt{3}r} \quad (15)$$

$$C_{44}^{SR} = \frac{1}{r^2}\left(\frac{dU_{FNN}}{dR}\right)_{R=r} + \frac{1}{r}\left(\frac{d^2U_{SNN}}{dR^2}\right)_{R=\sqrt{2}r} + \frac{3}{\sqrt{2}r^2}\left(\frac{dU_{SNN}}{dR}\right)_{R=\sqrt{2}r} + \frac{4}{3r}\left(\frac{d^2U_{TNN}}{dR^2}\right)_{R=\sqrt{3}r} + \frac{8}{3\sqrt{3}r^2}\left(\frac{dU_{TNN}}{dR}\right)_{R=\sqrt{3}r} \quad (16)$$

RESULTS AND CONCLUSION

The input data along with the corresponding references and calculated model parameters for BaSe and CeSe are given in TABLE 1 and 2, respectively. To study the phase transition properties of BaSe and CeSe, at first we have calculated the Gibbs free energy for B1 and B2 phase, and found that the calculated values of the Gibbs free energy at zero pressure (cohesive energy) in B1 phase is less than that of the B2 phase, which means B1 phase is thermodynamically and mechanically more stable than B2 phase. As the pressure increases, the difference of Gibbs free energy (*dG*) for two phases decreases and at the phase transition pressure it becomes zero. The difference of Gibbs free energy (*dG*) with pressure is plotted in Figures 1 and 2 for BaSe and CeSe, respectively. From these figures the phase transition pressure comes out to be 6.2 GPa for BaSe and 20.8 GPa for CeSe, which are in excellent agreement with the experimental findings[1,2]. The phase transition pressure, equilibrium separation for B2 phase, cohesive energies for B1 and B2 phase and relative volume at transition for B1 and B2 phase are given in TABLE 3, along with the experimental and other theoretical data.

The compression curve is calculated using the values of nearest neighbor separation $r(r^1)$ at different pres-

TABLE 1 : Input parameters

Crystal	r_0 (A^0)	B_0 (GPa)	% Volume collapse at transition
BaSe	3.2965 [1]	40.00 [4]	13.9 [1]
CeSe	2.9950 [2]	76.00 [2]	9.0 [2]

TABLE 2 : Calculated model parameters.

Crystal	$b_{B1}(10^{-19}J)$	$\rho_{B1}(A^0)$	$b_{B2}(10^{-19}J)$	$\rho_{B2}(A^0)$	% Decrease in range parameter for B2 phase
BaSe	916.4436	0.4840	1221.9248	0.4510	6.82
CeSe	4940.2330	0.3507	6586.9773	0.3371	3.88

TABLE 3 : Phase transition and cohesive properties.

Crys.	Equilibrium sep. for B2 phase r_0^1 (A^0)	Cohesive energy U_{B1} (kJ/Mol)	Cohesive energy U_{B2} (kJ/Mol)	P_T (GPa)	$V_T(B1)/V_0(B1)$	$V_T(B2)/V_0(B2)$
BaSe						
Prese.	3.43324	-2530.61	-2491.03	6.20	0.886	0.787
Exp.				6.00 [1]		
Other	3.35498 [10]			6.02 [10]	0.880 [10]	0.759 [10]
	5.50099 [5]			6.80 [5]	0.901 [5]	0.785 [5]
	3.37100 [7]			5.20 [7]	0.880 [7]	0.762 [7]
	5.37456 [6]			5.60 [6]	0.890 [6]	0.760 [6]
CeSe						
Prese.	3.15449	-2868.21	-2779.02	20.8	0.834	0.854
Exp.				20.0 [2]		
Other	3.14021 [15]	-2268.92 [15]	-2204.40 [15]	18.6 [15]	0.820 [11]	0.822 [11]
	3.14021 [11]			22.0 [11]		

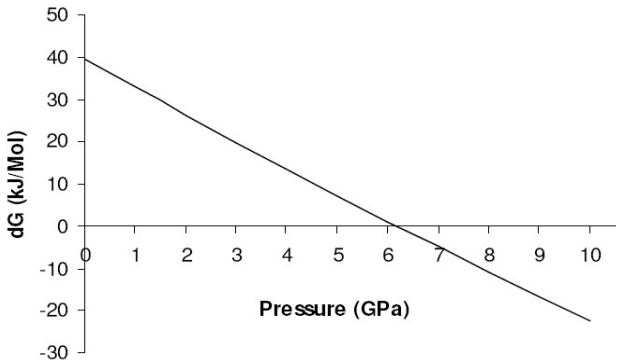

Figure 1 : The variation of the difference for Gibbs free energies (dG) in B1 and B2 phase with pressure for BaSe.

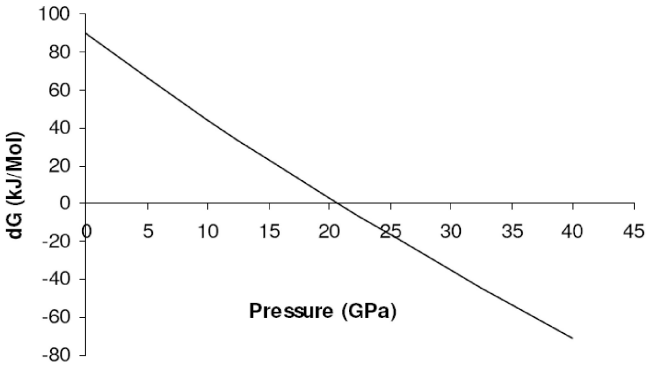

Figure 2 : The variation of the difference for Gibbs free energies (dG) in B1 and B2 phase with pressure for CeSe.

sure for BaSe and CeSe, and are plotted in the Figures 3 and 4, respectively. The experimental points are shown by filled triangles for the shake of compression. It is clear from these figures that our calculated results for compression curve are quite close to the available experimental data. From these figures it may also be noted that the B1-B2 phase transition occurs with discontinuity in volume at the phase transition pressure.

Figures 5 and 6 represents the variation of nearest neighbor distance i.e., Ba-Se (Ce-Se), and next nearest neighbor distance i.e., Ba-Ba (Ce-Ce), with pressure for BaSe and CeSe, respectively. From these figures it may be noted that the nearest neighbor separation increases, while the next nearest neighbor separation decreases at B1 to B2 transition. This may be explained by the mechanism of the B1-B2 transition in which the increase in pressure causes the unfolding of the bonding between the ions. At B1-B2 phase transition the Ba-Se distance increases by 0.155 A^0 while Ce-Se distance increases by 0.174 A^0. This increase can be interpreted as an increase of the cation radius at B1-B2 phase transition, because the anionic radius can be taken as independent of the crystal structure[22]. According to the stability criterion of B1 and B2 phase, the NaCl type structure becomes stable only if the ratio of cation radius to the anion radius is between 0.41 to

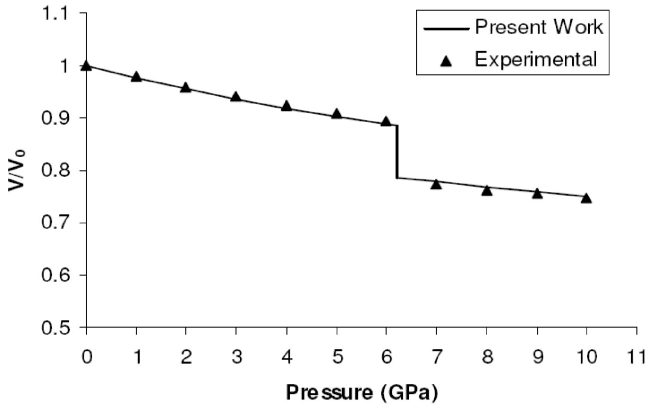

Figure 3 : Compression curve for BaSe. Exp. points are from ref. [3].

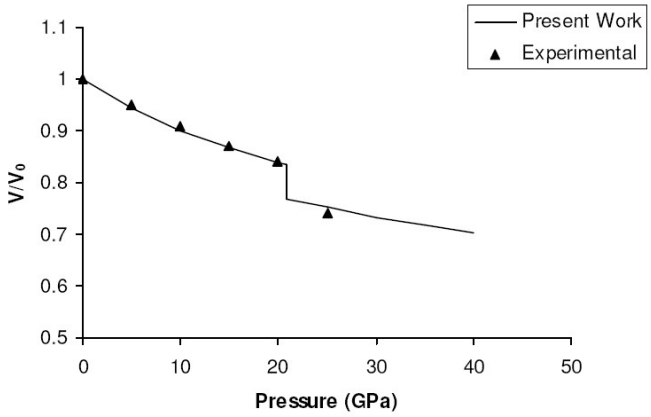

Figure 4 : Compression curve for CeSe. Exp. points are from ref. [2].

0.73 and the CsCl type structure becomes stable if the radius ratio is above 0.73[18,23]. Hence, our results also support the stability criterion of B1 and B2 phase and with the increase in cation radius for CsCl type structure, at the phase transition pressure the radius ratio crosses the critical value of 0.73 and the CsCl type structure becomes stable.

Calculated values of bulk modulus B_0 and the pressure derivative of bulk modulus B_0^1 for B1 and B2 phase

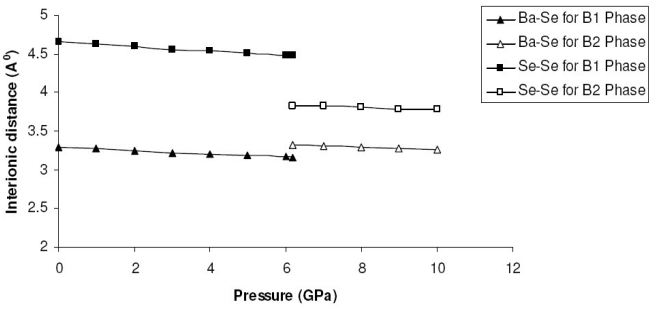

Figure 5 : Variation of interionic distances with pressure for BaSe.

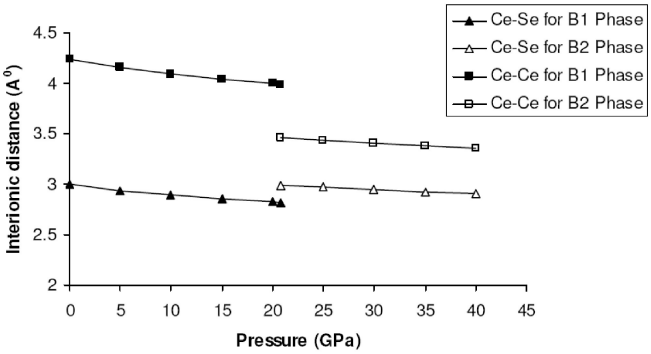

Figure 6 : Variation of interionic distances with pressure for CeSe.

are given in TABLE 4 along with other experimental and theoretical results. It can be reveal from TABLE 4 that our calculated values [from Vinet equation of state] of bulk modulus for B1 phase are quite close to the experimental values and hence verify the suitability of present potential model for BaSe and CeSe. It can also be seen from TABLE 4 that our calculated values [from eqn. (9)] of bulk modulus for B2 phase are greater than that of the B1 phase. This seems to be correct as the small lattice parameters generally lead to high bulk moduli[24] and is also consistent with the experimental work of H.G. Zimmer et al.[25] supported by their empirical relation for the bulk modulus of B2 phase, given as $B_{02} = B_{01}(V_{02}/V_{01})^{-1.1}$. Further, to check this result we have also calculated the bulk modulus for B2 phase from the thermodynamic condition $B_{02} = V_{02}\left(d^2U_{B2}(r^1)/dV_2^2\right)_{r^1=r_0^1}$ which gives

$$\mathbf{B_{02}} = \frac{\alpha_M^1 \mathbf{e}^2\mathbf{Z}^2}{4\pi\varepsilon_0 \times 4\sqrt{3}\left(\mathbf{r}_0^1\right)^4}\left[\frac{\mathbf{r}_0^1}{\rho_{B2}}\left\{\frac{\exp\left(\frac{-\mathbf{r}_0^1}{\rho_{B2}}\right)+\mathbf{e}4\exp\left(\frac{-2\sqrt{2}\mathbf{r}_0^1}{\sqrt{3}\rho_{B2}}\right)}{2\exp\left(\frac{-\mathbf{r}_0^1}{\rho_{B2}}\right)+2\sqrt{6}\exp\left(\frac{-2\sqrt{2}\mathbf{r}_0^1}{\sqrt{3}\rho_{B2}}\right)}\right\}-1\right] \quad (17)$$

Again, the values calculated from equation (17) shows that the bulk modulus for B2 phase is greater than that of the B1 phase for both BaSe and CeSe.

For NaCl phase the calculated values of second

Full Paper

TABLE 4 : Bulk modulus and its pressure derivative.

Crystal	Bulk Modulus from eqn. (9)		Bulk Modulus In B2 Phase (GPa), from eqn. (17)	B_0^1	
	In B1 Phase (GPa)	In B2 Phase (GPa)		In B1 phase	In B2 Phase
BaSe					
Present	40.04	47.92	55.96	4.05	4.99
Exp.	40.00 [4]				
Other	45.95 [10]	49.50 [10]		4.42 [10]	4.48 [10]
	41.29 [5]	39.46 [5]		3.74 [5]	3.58 [5]
	46.80 [6]	48.60 [6]		6.56 [6]	4.84 [6]
	45.41 [7]	52.90 [7]			
CeSe					
Present	75.44	86.70	90.38	4.77	5.37
Exp.	76.00 [2]			5.00 [2]	
Other	72.80 [15]	73.93 [11]		4.77 [11]	4.72 [11]
	74.39 [11]			5.20 [12]	
	83.40 [12]				

order elastic constants (SOEC) are given in TABLE 5 with available theoretical data. An inspection of TABLE 5 reveals that although the experimental values of the second order elastic constants for BaSe and CeSe are not available for the comparison, but the values of the bulk modulus predicted from these elastic constants by

TABLE 5 : Second order elastic constants for B1 phase.

Crystal	C_{11} (GPa)	C_{12} (GPa)	C_{44} (GPa)	B_{01} (GPa) from eqn. (18)
BaSe				
Present	45.94	37.02	37.02	39.99
Exp.				40.00
Other	99.34 [5]	8.29 [5]	8.38 [5]	38.64 [5]
	104.00 [10]	14.00 [10]	15.00 [10]	44.00 [10]
CeSe				
Present	130.36	48.81	48.81	75.99
Exp.				76.00 [2]
Other	198.93 [11]	10.22 [11]	93.40 [11]	73.12 [11]
	154.48 [15]	31.97 [15]	32.01 [15]	72.81 [15]

using the relation:

$$B_0 = \frac{1}{3}\left[C_{11} + 2C_{12}\right] \qquad (18)$$

are better than those of the previous workers as compared to the experimental values.

At last it is pertinent to mention here that to study the B1-B2 phase transition and elastic properties ab-inito calculations and some computer simulation programs like, WIEN2K are extensively being used. But the aim of the present study is to formulate the simple and straightforward potential model which determines the B1-B2 phase transition pressure, the equation of state (compression curve) and the elastic properties within the same accuracy as done by such rigorous calculations and computer codes. On the basis of overall description it may be concluded that the present potential model and its application in the present study has satisfactorily explained the structure stability, cohesive, elastic and phase transition properties of barium and cerium selenide which also validates the physical significance of range and strength parameters.

REFERENCES

[1] T.A.Grzybowski, A.L.Ruoff; Phys.Rev.B, **27**, 6502-6503 **(1983)**.

[2] J.M.Leger; Physica B, **190**, 84-91 **(1993)**.

[3] A.L.Ruoff, T.A.Grzybowski; Solid State Physics under Pressure, S.Minomura, (Ed); KTK Scientific Publishers, Tokyo, **(1985)**.

[4] A.Jayaraman, A.K.Singh, A.Chatterjee, S.U.Devi; Phy.Rev.B, **9**, 2513 **(1985)**.

[5] F.E.H.Hassan, H.Akbarzadesh; Computational Mater.Sci., **38**, 362-368 **(2006)**.

[6] S.H.Wei, H.Krakauer; Phys.Rev.Lett., **55**, 1200-1203 **(1985)**.

[7] G.Kalpana, B.Palanivel, M.Rajagopalan; Phys.Rev.B, **50**, 12318-12325 **(1994)**.

[8] K.Syassen, N.E.Christensen, H.Winzen, K.Fisher, J.Evers; Phys.Rev.B, **35**, 4052-4059 **(1987)**.

[9] A.E.Carlsson, J.W.Wilkins; Phys.Rev.B, **29**, 5836-5839 **(1984)**.

[10] A.Bouhemadou, R.Khenata, F.Zegrar, M.Sahnoun, H.Baltache, A.H.Reshak; Computational Mater.Sci., **38**, 263-270 **(2006)**.

[11] Bouhemadou, R.Khenata, M.Sahnoun, H.Baltache, M.Kharoubi; Physica B, **363**, 255-261 **(2005)**.

[12] Svane, W.Temmerman, Z.Szotek; Phys.Rev.B, **59**, 7888-7892 **(1999)**.

[13] P.K.Jha, U.K.Sakalle, S.P.Sanyal; J.Phys.Chem.Solids, **59**, 1633-1637 **(1998)**.

[14] P.Bhardwaj, S.Singh, N.K.Gaur; Cent.Eur.J.Phys., **6**, 223-229 **(2008)**.

[15] V.Srivastava, A.K.Bandyopadhyay, P.K.Jha, S.P.Sanyal; J.Phys.Chem.Solids, **64**, 907-912 **(2003)**.

[16] Kuldeep Kholiya, Swati Verma; Eur.Phys.J.B, 23-28 **(2011)**.

[17] Kuldeep Kholiya, Swati Verma; Phase Transitions, **84**, 67-76 **(2011)**.

[18] M.P.Tosi; Solid State Phys., **16**, 1-120 **(1964)**.

[19] Kuldeep Kholiya, B.R.K.Gupta; Physica B, **387**, 271-275 **(2007)**.

[20] P.Vinet, J.Ferrante, J.H.Rose, J.R.Smith; J.Geophys.Res., **92**, 9319 **(1987)**.

[21] A.J.Cohen, R.G.Gordon; Phys.Rev.B, **14**, 4593-4605 **(1976)**.

[22] R.D.Shannon, C.T.Prewitt; Acta Crystallogr.Sect.B, **25**, 925-946 **(1969)**.

[23] U.Benedict; J.Less Comm.Metals, **128**, 7-45 **(1987)**.

[24] M.S.S.Brooks, B.Johansson, H.L.Skriver, Handbook on the Physics and Chemistry of Actinides, A.J.Freeman, G.H.Lander, (Eds); Elsevier Science Publishers, New York, 230-265 **(1984)**.

[25] H.G.Zimmer, H.Winzen, K.Syassen; Phy.Rev.B, **22**,.4066-4070 **(1985)**.